Published in final edited form as:
Tree Physiol. 2011 January ; 31(1): 59–67. doi:10.1093/treephys/tpq099.

Cavitation in dehydrating xylem of *Picea abies*: energy properties of ultrasonic emissions reflect tracheid dimensions

Stefan Mayr[1,3] and **Sabine Rosner**[2]

[1]Department of Botany, University of Innsbruck, Sternwartestr. 15, A-6020 Innsbruck, Austria

[2]Department of Integrative Biology and Biodiversity Research, Institute of Botany, University of Natural Resources and Applied Life Sciences BOKU, Gregor-Mendelstr. 33, A-1180 Vienna, Austria

Abstract

Ultrasonic emission (UE) testing is used to analyse the vulnerability of xylem to embolism, but the number of UEs often does not sufficiently reflect effects on hydraulic conductivity. We monitored the absolute energy of UE signals in dehydrating xylem samples hypothesizing that (i) conduit diameter is correlated with UE energy and (ii) monitoring of UE energy may enhance the utility of this technique for analysis of xylem vulnerability. Split xylem samples were prepared from trunk wood of *Picea abies*, and four categories of samples, derived from mature (I: earlywood, II: 30–50% latewood, III: >50% latewood) or juvenile wood (IV: earlywood) were used. Ultrasonic emissions during dehydration were registered and anatomical parameters (tracheid lumen area, number per area) were analysed from cross-sections. Attenuation of UE energy was measured on a dehydrating wood beam by repeated lead breaks. Vulnerability to drought-induced embolism was analysed on dehydrating branches by hydraulic, UE number or UE energy measurements. In split samples, the cumulative number of UEs increased linearly with the number of tracheids per cross-section, and UE energy was positively correlated with the mean lumen area. Ultrasonic emission energies of earlywood samples (I and IV), which showed normally distributed tracheid lumen areas, increased during dehydration, whereas samples with latewood (II and III) exhibited a right-skewed distribution of lumina and UE energies. Ultrasonic emission energy was hardly influenced by moisture content until ~40% moisture loss, and decreased exponentially thereafter. Dehydrating branches showed a 50% loss of conductivity at −3.6 MPa in hydraulic measurements and at −3.9 and −3.5 MPa in UE analysis based on cumulative number or energy of signals, respectively. Ultrasonic emission energy emitted by cavitating conduits is determined by the xylem water potential and by the size of element. Energy patterns during dehydration are thus influenced by the vulnerability to cavitation, conduit size distribution as well as attenuation properties. Measurements of UE energy may be used as an alternative to the number of UEs in vulnerability analysis.

Keywords

earlywood; latewood; *Picea abies*; signal energy; tracheid dimension; ultrasonic emission; vulnerability to xylem embolism

[3]Corresponding author (stefan.mayr@uibk.ac.at).

Europe PMC Funders Author Manuscripts

Introduction

Terrestrial plant life depends on balanced water relations and thus on an efficient and intact water transport system, besides sufficient water uptake, stomatal control and water storage. Xylem embolism (e.g., Tyree et al. 1994, Hacke and Sperry 2001, Tyree and Zimmermann 2002) can dramatically reduce the water supply to distal tissues, amplify drought stress and, in the worst case, lead to fatal 'run-away embolism' (Tyree and Sperry 1988). Embolized conduits reduce the hydraulic conductivity of xylem. A plant's vulnerability to drought-induced embolism can be analysed by vulnerability curves (VCs) relating the percentage loss of hydraulic conductivity (PLC) of xylem to the pressure potential (P) in xylem sap (Sperry et al. 1988). The PLC is measured by hydraulic techniques (reviewed in Cruiziat et al. 2002, Tyree and Zimmermann 2002, Cochard 2006), but these methods are destructive. While first methodical approaches were also time intensive, innovative hydraulic measurement systems meanwhile enabled vulnerability analysis to be speeded up (Alder et al. 1997, Cochard 2002, Cochard et al. 2005, Li et al. 2008).

Ultrasonic emission (UE) testing can also be used for vulnerability analysis, and much effort has been made to refine UE analysis methods (Laschimke et al. 2006, Rosner et al. 2006, 2009, Johnson et al. 2009). This was enabled by a new digital generation of UE testing equipment and sophisticated software tools capable of measuring and analysing waveform features of the enormous number of ultrasound signals emitted during wood dehydration (Beall 2002, Vallen 2002). The advantage of the acoustic method is that it is non-destructive, allows real-time registration of cavitation events and is readily automated; the disadvantage, however, is that data interpretation is difficult in some woody species, especially in angiosperms (Tyree and Dixon 1986, Hacke and Sauter 1995, Hacke and Sauter 1996).

Embolism formation is induced by air-seeding processes, when air enters water-filled conduits from adjacent, already air-filled spaces (i.e., cavitation; e.g., Sperry and Tyree 1990, Tyree et al. 1994, Hacke and Sperry 2001, Tyree and Zimmermann 2002). In contrast to hydraulic methods, UE testing does not enable quantification of the effects of embolism formation on hydraulic conductivity, but monitoring of cavitation events themselves. The bulk of UEs in dehydrating wood are supposed to be induced by cavitation, i.e., by the rapid tension release in the conduit lumen when liquid water at negative pressure is replaced by water vapour near vacuum pressure (Tyree et al. 1984b, Sandford and Grace 1985, Tyree and Sperry 1989*a*, 1989*b*, Kawamoto and Williams 2002, Rosner et al. 2006; also see Cochard and Tyree 1990, Kikuta 2003).

The plant physiological application of UE testing focuses mainly on counting all UE signals surpassing a defined detection threshold, on the assumption that the cumulative UE number corresponds to a loss in hydraulic conductivity (Tyree and Dixon 1983, Tyree et al. 1984*a*, Lo Gullo and Salleo 1991, Cochard 1992). The construction of VCs based on UE counting and the corresponding P is complicated by the fact that any (dead) water-filled cell with walls rigid enough to resist collapse under negative pressure is capable of cavitation (Tyree and Sperry 1989*a*, Kikuta 2003). Ultrasonic emissions can thus originate in drought-stressed plants from conducting and non-conducting wood elements (Sandford and Grace 1985, Tyree and Dixon 1986) and from bark tissue (Kikuta 2003). The cumulative rate of UEs is, therefore, not always proportional to the PLC, because cavitations of non-conductive cells are also counted. Even if each single signal represented exactly one cavitation event in a conduit (Tyree and Dixon 1983, Tyree et al. 1984*a*), the relationship between cumulative UEs and conductivity loss will be non-linear if not all of the xylem elements individually contribute the same amount to the total hydraulic conductivity (Cochard 1992). Furthermore, acoustic coupling of sensors to the xylem, varying inhomogeneous xylem areas and

attenuation effects, e.g., caused by variation in wood density and xylem water content, may affect UE analysis.

In consequence, VCs based on ultrasonic measurements often differ from reference hydraulic curves, so that there is a need and probably potential to improve and optimize UE analysis. Recently, a method for constructing VCs of Norway spruce trunk wood was presented, where the cumulative amount of UE energy, a waveform feature corresponding to the signal strength, was used (Rosner et al. 2006, 2009). Results indicated that the course of UE energy may be a better estimate for the PLC than UE counts *per se*. Comparison of adult and juvenile wood samples suggested that wider conduits emit UEs of higher energy so that the use of UE energy might enable improved weighting of UE events according to the hydraulic function of failed conduits. However, adult and juvenile samples showed a broad range of tracheid dimensions so that proof of the correlation of conduit dimensions and UE energy is still lacking. Furthermore, VCs in Rosner et al. (2009) were based on air injection experiments, and *P* in Rosner et al. (2006) was estimated via relative water content. We do not know whether air injection and natural dehydration cause identical UE properties and whether the use of water content may lead to artificial shifts in VCs. Thus, measurements of UE energy and *P* on dehydrating branches would be required to estimate a possible use in vulnerability analysis.

In the present study, we thus followed two main goals: first, the suggested positive correlation between transverse tracheid dimension and UE energy should be tested. We therefore analysed UEs during dehydration of *Picea abies* xylem samples, which were categorized in four groups differing in size and frequency distribution of tracheid cross-sectional area. Second, vulnerability analysis on intact dehydrating branches of *P. abies*, based on the number of UEs as well as UE energy, should be established and compared with hydraulic vulnerability analysis. We hypothesized that the use of UE energy may improve vulnerability analysis.

Materials and methods

Sample preparation

Wood for the preparation of defined split samples and attenuation analysis came from four 25-year-old Norway spruce trees (*P. abies* (L.) Karst.) of a clonal trial in Southern Sweden (described in Rosner et al. 2009). Wood specimens were taken immediately after felling at the tree top (second internode) and at 1 m height from the ground. Small wood specimens split along the grain (0.7 mm radial, 4.0 mm tangential and 17.0 mm longitudinal) with defined wood anatomy were produced from the outer sapwood taken at 1 m from the ground (annual rings 17–19, mature wood) and at the tree top (annual rings 1–2, juvenile wood). The 0.7-mm radial file of Category I wood splits consisted of mature earlywood of quite uniform tracheid diameter (Figure 1a), Category II of wood from the earlywood–latewood transition zone or of mature earlywood with 30–50% latewood from the previous annual ring (Figure 1d), Category III of mature wood with >50% latewood from the previous or the same annual ring (Figure 1g) and Category IV of juvenile earlywood of quite uniform tracheid diameter (Figure 1j). Wood splits were produced using a self-made microtome blade tool. The advantage of wood splitting compared with cutting is that possible transverse severing of the tracheids can be avoided. During all preparation steps, samples were kept wet until they were soaked in distilled water under vacuum for at least 24 h to refill embolized tracheids (Hietz et al. 2008).

To test the relationship between UE energy and moisture content, a spruce beam of mature wood with dimensions 150 mm (axial) × 7 mm (radial) × 10 mm (tangential) was produced

on a sliding microtome. The wood beam was saturated in distilled water under vacuum for at least 24 h (Hietz et al. 2008).

For vulnerability analysis, Norway spruce branches were harvested in Natters, Austria (11°21'E, 47°14'N, 838 m). Branches ~1.5 m long and 5–10 years old were cut from 5-m high trees at breast height, immediately wrapped in plastic bags and transported to the laboratory of the Institute of Botany in Innsbruck. Branches were re-cut under water and saturated for at least 12 h.

Ultrasonic emission analysis on dehydrating split wood samples

Ultrasonic emissions were monitored with the μDiSP™ Digital AE system (Physical Acoustics Corporation, Princeton Jct, PA, USA). Preamplifiers (40 dB) were used with resonant 150-kHz R15C transducers over the standard frequency range of 50–200 kHz. Ultrasonic emissions were recorded with a detection threshold of 30 dB (0 dB = 1 μV input). Extraction of the absolute UE energy (aJ) of each UE signal was carried out with AE Win® software (Physical Acoustics Corporation). The absolute energy is derived from the integral of the squared voltage signal divided by the reference resistance over the duration of an acoustic signal (Manual for PCI-2 system; Physical Acoustics Corporation, 2007). The acoustic transducer was positioned on the tangential split face of the fully saturated wood specimen using an acrylic resin clamp construction (Rosner et al. 2009), which enables the contact pressure of the acoustic transducer to be set to a nearly constant value of 30.0 ± 1.0 N (Jackson and Grace 1996, Beall 2002). Silicone paste (Wacker, Burghausen, Germany) served as a coupling agent. Acoustic emission testing was performed till the cessation of all acoustic activity, which took <10 h. Thereafter, dry weight (DW) of the wood splits was obtained by drying at 103 °C to constant weight for calculation of wood density.

Energy of ultrasonic signals in dependence of moisture content

The change in UE energy with increasing moisture loss was tested via lead breaks on a fully saturated fresh Norway spruce wood beam with dimensions 150 mm (axial) × 7 mm (radial) × 10 mm (tangential). Lead breaks are a standard method (HSU-Nielsen lead break) of creating UEs with relatively constant signal strength. They can be used to test sensors or attenuation properties of a material. For tests, a retractable pencil is positioned on the material with the lead (5 mm, 2H) protruding ~3 mm from the pencil tip. The pencil is then gently pressed on the material at an angle of ~45° until the lead breaks and produces a UE signal. When the distance between the position at which the lead break is produced and the sensor is constant, the strength of registered signals decreases with increasing attenuation. In this study, the distance between UE transducer (R15, PAC) and the HSU-Nielsen lead break source (5 mm, 2H) was 10 cm. Lead breaks were performed at variable relative moisture loss steps from 0 to 96%. Dry weight was determined after drying at 103 °C to constant weight. Relative moisture loss was calculated as

$$\left(1 - \frac{\mathrm{FW} - \mathrm{DW}}{\mathrm{SW} - \mathrm{DW}}\right) \times 100 \quad (1)$$

where FW is the fresh weight at variable moisture loss and SW is the saturated weight.

Vulnerability analysis on dehydrating branches based on ultrasonic measurements

Saturated branches were dehydrated on the bench, while UEs from the main axes were recorded and, at intervals, P of a terminal twig was determined. Branches were taken out of plastic bags, and at the upper side (opposite wood) of the axes, ~10 cm from the base, ~3 cm^2 of the bark were removed and the xylem was covered with silicone paste (to improve acoustic coupling and prevent transpiration), before R15C sensors were attached with

clamps (metal springs coated by plastic material). Sensors were connected to a 20/40/60 dB preamplifier set to 40 dB and to a PCI-2 system (PAC 125 18-bit A/D, 3 kHz–3 MHz PCI2; all components of the UE system from Physical Acoustics Corporation).

Registration and analysis of UEs were done with AEwin software (Physical Acoustics Corporation). Note that in these experiments, the contact area between sensor and sample cannot be controlled. Thus, the effective coupling pressure, which influences the intensity of registered signals, could neither be adjusted nor determined (also see Mayr and Sperry 2010). With branches, artificial signals in the low-amplitude range were frequently observed so that the threshold had to be set to 35 dB (0 dB = 1 μV input) and thus slightly higher compared with the split samples.

P was measured with a pressure chamber (Model 1000 Pressure Chamber; PMS Instrument Company, Corvallis, OR, USA) on ~5-cm long terminal twigs of branches. Twigs were carefully cut from dehydrating branches so that no artificial UEs were caused. Measured values were assumed to be similar to *P* of the main axis xylem as transpiration was low.

For vulnerability analysis, the cumulative number or energy of UEs corresponding to the measured *P* was related to the total number or energy of UEs until 4 days of dehydration at the bench. Vulnerability curves (UE parameter plotted against *P*) were fitted with an exponential sigmoidal equation (Pammenter and Vander Willigen 1998):

$$\text{cumulative UE parameter}\,(\%) = \frac{100}{1 + \exp\left(a\left(P - P_{50}\right)\right)} \quad (2)$$

where the cumulative UE parameter (number or energy of signals) is in %, *P* is the corresponding xylem pressure and parameter *a* is related to the curve slope. P_{50} corresponds to *P* at 50% of the maximum UE value. The VC was calculated using Fig.P 2.98 (Biosoft Corp., Cambridge, UK).

Vulnerability analysis on dehydrating branches based on hydraulic measurements

Loss of hydraulic conductivity was measured in saturated branches, which were dehydrated to different *P* at the bench. *P* was determined on three terminal twigs with the Scholander technique (see vulnerability analysis based on ultrasonic measurements). Average *P* was assumed to be similar to *P* of the main axis xylem.

The PLC was quantified by measuring the increase in hydraulic conductivity after removal of xylem embolism by repeated high-pressure flushes (Sperry et al. 1988). Samples up to 8 mm in diameter and up to 4 cm in length were prepared as described in Mayr et al. (2002). Measurement pressure was set to 4 kPa. The flow rate was determined with a PC-connected balance (Sartorius BP61S, 0.1 mg precision; Sartorius AG, Göttingen, Germany) by recording weight every 10 s and fitting linear regressions over 200-s intervals. Flushing (at 80 kPa) and conductivity measurements were done with distilled, filtered (0.22 μm) and degassed water containing 0.005% (v/v) ‘Micropur’ (Katadyn Products Inc., Wallisellen, Switzerland) to prevent microbial growth. Flushing was repeated until measurements showed no further increase in conductivity. The PLC was calculated from the ratio of initial to maximal conductivity (Sperry et al. 1988). Vulnerability curves (PLC versus *P*) were fitted according to equation (2) with ultrasonic parameter substituted by PLC. The PLC of one to four samples per branch was measured and the average value used for vulnerability analysis. The VC was calculated using Fig.P 2.98 (Biosoft Corp.).

Anatomical analysis

Wood splits were re-soaked in a mixture of distilled water, ethanol and glycerin (1:1:1). Transverse sections with a thickness of 20 μm were prepared on a sliding microtome. Sections were stained with methylene blue and mounted in Euparal (Merck, Darmstadt, Germany). Tagged image files of 0.7 mm (radial) × 0.5 mm (tangential) reference windows were made with a Leica DM4000M microscope interfaced with a digital camera (Leica Microsystems Wetzlar GmbH, Germany). Transverse lumen areas, radial and tangential lumen diameters of each tracheid within the reference window were measured by National Institutes of Health (NIH) Image software (freely available from http://rsb.info.nih.gov).

Number of samples and statistics

For experiments with split wood samples, the number of replicates for Categories I, II, III and IV was 10, 10, 8 and 10. For observations on the relationship between UE energy and moisture content, eight lead breaks per moisture loss step were performed on a wood beam. Three branches were used for vulnerability analysis based on the acoustic method and PLC measurements were from 55 branches. Differences were tested with Student's *t*-test, ANOVA and subsequent Scheffé test. Testing of hydraulic versus UE vulnerability parameters was not possible as statistical units differ: each data point in the hydraulic vulnerability represents measurements on one branch, and parameters were calculated from the mean sigmoidal curve. In UE measurements, curves for each branch and, subsequently, the average of curve parameters were calculated. Correlation coefficients (hydraulic versus anatomical parameters of all samples) were tested with Pearson's product–moment coefficient. All tests (two-tailed) were performed pairwise at a probability level of 5% using SPSS (Ver. 15.0, SPSS Inc., Chicago, IL, USA).

Results

Anatomy of split wood samples and UE during dehydration

Wood splits of mature (Category I, Figure 1c) and juvenile earlywood (Category IV, Figure 1l) emitted higher UE energies towards the end of dehydration. Mean lumen areas of these specimens were normally distributed (Figure 1b and k). Mature wood splits from the earlywood–latewood transition zone or wood splits that contained <50% of latewood (Category II) and mature wood splits with a high percentage of latewood (Category III) showed a right-skewed distribution of lumen areas (Figure 1e and h) and UE energy (Figure 1f–i). Absolute mean values of lumen area and UE energies were much higher in Category II than in Category III samples (Table 1). The largest radial and tangential lumen diameters and lowest numbers of tracheid transverse area were found in Category I specimens (Table 1). Juvenile wood splits (Category IV) and splits with >50% latewood (Category III) had the smallest tracheids and highest tracheid numbers per cross-sectional area. The total number of UEs was strongly linearly related to the number of tracheids per square millimetre (Figure 2a). Although the highest tracheid numbers per cross-sectional area were found in juvenile wood, wood density had highest values in specimens with a high percentage of latewood (Table 1). Mean lumen area and UE energy showed quite similar values in Category III and IV wood splits; and both parameters were significantly lower than in Category I and II wood splits. Ultrasonic emission energies were, therefore, strongly related to tracheid lumen areas across categories (Figure 2b).

Energy changes of ultrasonic signal with varying wood moisture

Below 40% relative moisture loss, evaporative water loss did not lead to a significant decrease in signal strength as indicated by similar absolute energy values of the lead break source. The absolute energy of the acoustic signal from the lead break increased, however,

exponentially after 60% relative moisture loss (Figure 3), indicating a significant decrease in attenuation at higher moisture losses ($P < 0.001$).

Vulnerability analysis on dehydrating branches

All VCs showed a sigmoid shape (Figure 4), whereby parameter *a*, which indicates the slope of curves, was higher with hydraulic measurements than with ultrasonic measurements (Table 2). P_{50} was lowest in VCs based on the cumulative number of acoustic events and highest in curves from UE energy analysis, where the latter had quite similar values to those obtained by the hydraulic method. P_{12} was less negative when obtained with UE energy than with UE counting or by the hydraulic method.

During dehydration, the energy of UEs increased at the beginning and peaked when ~15% of all UE signals were emitted (Figure 5). Mean energy of UEs at this time was >300 aJ. During further dehydration, UE energy decreased to ~100 aJ (when ~80% of all signals were emitted) and showed a slight increase at the end of the dehydration procedure.

Discussion

The signal strength of UEs released by a cavitating xylem element can be influenced by several factors, associated with wood structure and moisture content. In this study, the absolute energy, defined as the integral of the squared voltage signal divided by the reference resistance over the duration of an acoustic signal, was used as an estimate for signal strength of UEs related to xylem cavitation.

Ultrasonic emission energy should be linearly correlated with *P* of xylem sap because higher negative pressure of water columns causes higher energy release on breakage of columns (Tyree and Sperry 1989*b*). Ultrasonic emission energy set free by cavitation also depends on the volume of xylem elements. Assuming that cavitation occurs conduit by conduit, larger elements will release more energy than smaller ones (Rosner et al. 2006, 2009, Johnson et al. 2009). Thus, UE energy theoretically can be calculated as the product of the fluid's volume and the fluid's *P* in a cavitating xylem element. However, as UE detection and analysis is strongly influenced by a material's attenuation, an interpretation of UE properties is very difficult in wood, which represents an acoustically inhomogeneous material: besides differences in sound propagation in the three wood directions (Beall 2002, Kawamoto and Williams 2002), attenuation is influenced by wood density (Ritman and Milburn 1988, Tyree and Sperry 1989*b*, Jackson and Grace 1996, Kawamoto and Williams 2002) and by the xylem water content (Ritman and Milburn 1988, Tyree and Sperry 1989*a*, Quarles 1990, Jackson and Grace 1996, Beall 2002). We suppose that anatomical properties (resin canals, ray cells, cell wall thickness, cell wall microstructure, pit structures, etc.) may influence attenuation as well. Thus, in an entire branch, with latewood and earlywood, reaction wood, reorganization at branch junctions, etc., complex interrelations of UE energy patterns and wood properties have to be expected.

In this study, the preparation of wood splits enabled the analysis of UE signals in defined xylem samples: tracheid size (lumen area and diameter) decreased from Category I to Category IV, and, accordingly, the number of tracheids per cross-sectional area increased (Table 1). Categories also differed in tracheid area distribution with normally distributed areas in earlywood samples (Categories I and IV) and right-skewed distribution in samples containing latewood portions (Categories II and III; Figure 1).

According to variation in anatomical properties, we observed significant differences in the quantity and energy of ultrasonic activity during dehydration.

Europe PMC Funders Author Manuscripts

i. The total number of UEs increased with the number of tracheids in a cross-sectional area (Table 1, Figure 2). Several authors observed a positive correlation between the number of tracheids and the number of UEs (Tyree and Dixon 1983, Tyree et al. 1984*a*, Sandford and Grace 1985, Cochard 1992), which indicates that cavitations occur tracheid by tracheid or in grouped tracheids with a similar number of elements per group.

ii. The mean energy of UE signals was correlated with the lumen area (Table 1, Figure 2), which corresponds to results presented in Rosner et al. (2009). Interestingly, the observed relationship was best fitted by a quadratic function (Figure 2). This may be explained by an increase in attenuation of wood with wide tracheids and thus low density (Ritman and Milburn 1988, Tyree and Sperry 1989*a*, Jackson and Grace 1996).

iii. As shown in Figure 1, there are also remarkable differences in the temporal pattern of UE energies on dehydration. In the case of normally distributed tracheid lumina (Categories I and IV), UE energies increased until >90% of all UEs were emitted. At the end of dehydration, UE energies decreased. In these homogeneous xylem samples, UE energy was probably determined primarily by *P*. During dehydration, *P* decreased and thus the tensile energy stored in water columns increased. We assume that changes in attenuation due to decreasing water content played a minor role: as demonstrated in Figure 3, energy of UEs produced by lead breaks hardly decreased between 0 and 40% relative water loss, which is the physiologically relevant range (see Rosner et al. 2009). This indicates that effects of dehydration on attenuation of UEs caused by embolism formation were small too. Note that it is only an indication as attenuation is a function of signal frequency, material properties and travelling distance of the acoustic wave. For this reason, attenuation analysed with lead breaks also cannot be used to correct signal strength of UEs caused by embolism during dehydration. The low energies observed towards the end of dehydration (Figure 1, 95–100% cumulative UE) might be caused by cavitation of very small (but resistant) tracheids, intercellular cavities in the xylem or ray tracheids (Rosner et al. 2006). In contrast, Categories II and III showed a peak in UE energy, when ~30% of all signals were emitted. Energies during the consecutive dehydration decreased slowly and reached lowest values with the last signals (Figure 1). According to the correlation of lumen area and UE energy (Figure 2), we suggest that earlywood tracheids within these samples were more vulnerable and cavitated first (at less negative *P*), leading to the release of high-energy UE due to large tracheid volumes. Latewood tracheids cavitated at the end of dehydration, at more negative *P*. Despite negative *P*, energies of single UEs at this stage were low as cavitation occurred in tracheids with small volumes. As shown in Table 1, the mean UE energy of specimens containing large amounts of latewood (Category III) was, therefore, smaller than in pure earlywood specimens (Category I).

In entire branches, wood composition is complex and tracheid size varies considerably. According to the Hagen–Poiseuille equation, tracheid size has major hydraulic consequences. This aspect is ignored when UE counts are used in vulnerability analysis so that differences between curves from hydraulic and acoustic measurements have to be expected (e.g., LoGullo and Salleo 1991, Cochard 1992, Rosner et al. 2006, Pittermann and Sperry 2006, Mayr and Sperry 2010). In our study, *P. abies* branches showed a lower P_{50} when based on UE counts compared with measurements with the hydraulic method (Figure 4, Table 2). In contrast, the use of UE energy in vulnerability analysis revealed a P_{50} that was only 0.14 MPa higher than in the hydraulic curve. This is caused by the fact that wider tracheids emit more energy and thus contribute more to the curve of cumulative UE energy

than smaller tracheids. Thus, the use of UE energy instead of UE counts may enable the weighting of cavitation events to be improved, and UE information and hydraulic conductivity of cavitated conduits to be matched.

Nevertheless, UE counting resulted in a better estimate for P_{12} than the UE energy method although UE had started already when there was no measurable decrease in PLC. We explain the latter by cavitations in drought-stressed needles adjacent to the UE sensor and by xylem wounding. To position the UE sensor properly on the xylem, the bark has to be removed. The best sealing material (which cannot be applied on a wet wood surface) does not prevent evaporative losses as this is provided by an intact periderm. We therefore suppose that cavitation occurred locally (near the UE sensor) already at an earlier stage of dehydration as in the bench-dehydrated branches used for PLC measurements. This local drought stress might then lead to relatively high UE energies when cavitation of large diameter tracheids takes place. For further studies, we suggest that great care be taken when sealing the small wounds around the UE sensor. One strategy could also be to cut away the bark, position the UE sensor, seal the wound properly and let the branch saturate again for some hours before the dehydration experiment is started.

The course of UE energy during dehydration may also give information on the size of elements cavitated. Figure 5 shows an initial peak (at 15% of all emitted UEs) in UE energy, which might reflect cavitation of the widest tracheids. The consecutive UE energy decrease indicates that cavitation occurs more frequently in smaller tracheids. This obviously masked the effect of decreasing P until ~80% of all signals were emitted. The size of the smallest elements and cavities in the wood was probably very similar so that the increase in UE energy related to the decrease in P can be seen during this last stage of dehydration.

Conclusions

Ultrasonic emission energy emitted by a cavitating conduit is influenced by the size of the element and P in the xylem, whereby P inducing cavitation of an element depends on the element's vulnerability threshold. The variability in vulnerability and the distribution of conduit size within a wood sample thus determine the pattern of UE energy during dehydration. Measurements of UE energy may improve vulnerability analysis, but, as weighting of acoustic signals via energy reflects many complex and interrelated factors, test measurements for each species are recommended. Ultrasonic emission energy analysis may be especially useful in vulnerability analysis of gymnosperms while difficulties with the interpretation of UEs from inhomogeneous angiosperm wood have to be expected.

Acknowledgments

We thank Mag. Verena Zublasing for participation in measurements and Mag. Ing. Birgit Dämon for excellent assistance.

Funding

This study was supported by APART (Austrian programme for advanced research and technology) and FWF (Fonds zur Förderung der Wissenschaftlichen Forschung).

References

Alder NN, Pockman WT, Sperry JS, Nuismer S. Use of centrifugal force in the study of xylem cavitation. J. Exp. Bot. 1997; 48:665–674.

Beall FC. Overview of the use of ultrasonic technologies in research on wood properties. Wood Sci. Technol. 2002; 36:197–212.

Cochard H. Vulnerability of several conifers to air embolism. Tree Physiol. 1992; 11:73–83. [PubMed: 14969968]

Cochard H. A technique for measuring xylem hydraulic conductance under high negative pressures. Plant Cell Environ. 2002; 25:815–819.

Cochard H. Cavitation in trees. C. R. Phys. 2006; 7:1018–1026.

Cochard H, Tyree MT. Xylem dysfunction in *Quercus*: vessel sizes, tyloses, cavitation and seasonal changes in embolism. Tree Physiol. 1990; 6:393–407. [PubMed: 14972931]

Cochard H, Damour G, Bodet C, Tharwat I, Poirier M, Améglio T. Evaluation of a new centrifuge technique for rapid generation of xylem vulnerability curves. Physiol. Plant. 2005; 124:410–418.

Cruiziat P, Cochard H, Améglio T. Hydraulic architecture of trees: main concepts and results. Ann. For. Sci. 2002; 59:723–752.

Hacke UG, Sauter JJ. Vulnerability of xylem to embolism in relation to leaf water potential and stomatal conductance in *Fagus sylvatic*a f. *purpurea* and *Populus balsamifera*. J. Exp. Bot. 1995; 46:1177–1183.

Hacke UG, Sauter JJ. Drought-induced xylem dysfunction in petioles, branches, and roots of *Populus balsamifera* L. and *Alnus glutinosa* (L.). Gaertn. Plant Physiol. 1996; 111:413–417.

Hacke UG, Sperry JS. Functional and ecological xylem anatomy. Persp. Plant Ecol. Evol. Syst. 2001; 4:97–115.

Hietz P, Rosner S, Sorz J, Mayr S. Comparison of methods to quantify loss of hydraulic conductivity in Norway spruce. Ann. For. Sci. 2008; 65:502–508.

Jackson GE, Grace J. Field measurements of xylem cavitation: are acoustic emissions useful? J. Exp. Bot. 1996; 47:1643–1650.

Johnson DM, Meinzer FC, Woodruff DR, McCulloh KA. Leaf xylem embolism, detected acoustically and by cryo-SEM, corresponds to decreases in leaf hydraulic conductance in four evergreen species. Plant Cell Environ. 2009; 32:828–836. [PubMed: 19220781]

Kawamoto, S.; Williams, RS. Acoustic emission and acousto-ultrasonic techniques for wood and wood-based composites: a review. U.S. Department of Agriculture, Forest Service, Forest Products Laboratory; Madison, WI: 2002. p. 1-16.Gen. Techn. Rep. FPL-GTR-134

Kikuta SB. Ultrasound acoustic emissions from bark samples differing in anatomical characteristics. Phyton. 2003; 43:161–178.

Laschimke R, Burger M, Vallen H. Acoustic emission analysis and experiments with physical model systems reveal a peculiar nature of the xylem tension. J. Plant Physiol. 2006; 163:996–1007. [PubMed: 16872717]

Li Y, Sperry JS, Taneda H, Bush SE, Hacke UG. Evaluation of centrifugal methods for measuring xylem cavitation in conifers, diffuse- and ring-porous angiosperms. New Phytol. 2008; 177:558–568. [PubMed: 18028295]

Lo Gullo MA, Salleo S. Three different methods for measuring xylem cavitation and embolism: a comparison. Ann. Bot. 1991; 67:417–424.

Mayr S, Sperry JS. Freeze–thaw-induced embolism in *Pinus contorta*: centrifuge experiments validate the ‘thaw-expansion hypothesis’ but conflict with ultrasonic emission data. New Phytol. 2010; 185:1016–1024. [PubMed: 20028475]

Mayr S, Wolfschwenger M, Bauer H. Winter-drought induced embolism in Norway spruce (*Picea abies*) at the Alpine timberline. Physiol. Plant. 2002; 115:74–80. [PubMed: 12010469]

Pammenter NW, Vander Willigen C. A mathematical and statistical analysis of the curves illustrating vulnerability of xylem to cavitation. Tree Physiol. 1998; 18:589–593. [PubMed: 12651346]

Pittermann J, Sperry JS. Analysis of freeze–thaw embolism in conifers. The interaction between cavitation pressure and tracheid size. Plant Physiol. 2006; 140:374–382. [PubMed: 16377751]

Quarles SL. The effect of moisture content and ring angle on the propagation of acoustic signals in wood. J. Acoust. Emission. 1990; 9:189–195.

Ritman KT, Milburn JA. Acoustic emissions from plants: ultrasonic and audible compared. J. Exp. Bot. 1988; 38:1237–1248.

Rosner S, Klein A, Wimmer R, Karlsson B. Extraction of features from ultrasound acoustic emissions: a tool to assess the hydraulic vulnerability of Norway spruce trunkwood? New Phytol. 2006; 171:105–116. [PubMed: 16771986]

Rosner S, Karlsson B, Konnerth J, Hansmann C. Shrinkage processes in standard-size Norway spruce wood specimens with different vulnerability to cavitation. Tree Physiol. 2009; 29:1419–1431. [PubMed: 19797244]

Sandford AP, Grace J. The measurement and interpretation of ultrasound from woody stems. J. Exp. Bot. 1985; 36:298–311.

Sperry JS, Tyree MT. Water-stress-induced xylem embolism in three species of conifers. Plant Cell Environ. 1990; 13:427–436.

Sperry JS, Donnelly JR, Tyree MT. A method for measuring hydraulic conductivity and embolism in xylem. Plant Cell Environ. 1988; 11:35–40.

Tyree MT, Dixon MA. Cavitation events in *Thuja occidentalis* L.? Ultrasonic acoustic emissions from the sapwood can be measured. Plant Physiol. 1983; 72:1094–1099. [PubMed: 16663126]

Tyree MT, Dixon MA. Water stress induced cavitation and embolism in some woody plants. Physiol. Plant. 1986; 66:397–405.

Tyree MT, Sperry JS. Do woody plants operate near the point of catastrophic xylem dysfunction caused by dynamic water stress? Plant Physiol. 1988; 88:574–580. [PubMed: 16666351]

Tyree MT, Sperry JS. Vulnerability of xylem to cavitation and embolism. Annu. Rev. Plant Physiol. Plant Mol. Biol. 1989a; 40:19–38.

Tyree MT, Sperry JS. Characterization and propagation of acoustic emission signals in woody plants: towards an improved acoustic emission counter. Plant Cell Environ. 1989b; 12:371–382.

Tyree, MT.; Zimmermann, MH. Xylem structure and the ascent of sap. Springer; Berlin: 2002.

Tyree MT, Dixon AD, Tyree EL, Johnson R. Ultrasonic acoustic emissions from the sapwood of cedar and Hemlock. An examination of three hypothesis regarding cavitations. Plant Physiol. 1984a; 75:988–992. [PubMed: 16663774]

Tyree MT, Dixon MA, Thompson RG. Ultrasonic acoustic emissions from the sapwood of *Thuja occidentalis* measured inside a pressure bomb. Plant Physiol. 1984b; 74:1046–1049. [PubMed: 16663501]

Tyree MT, Davis SD, Cochard H. Biophysical perspectives of xylem evolution: is there a tradeoff of hydraulic efficiency for vulnerability to dysfunction? IAWA J. 1994; 15:335–360.

Vallen H. AE testing fundamentals, equipment, applications. 2002; 7:1–29. NDT.net.

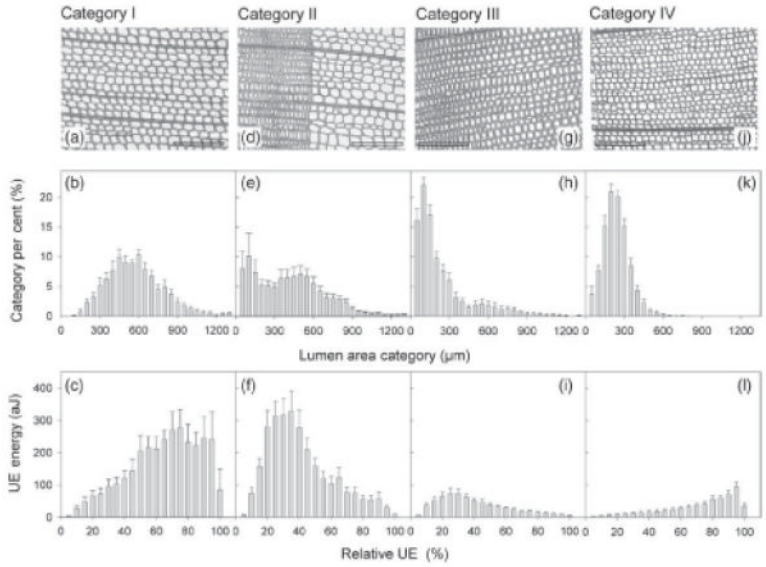

Figure 1.

Anatomy of split samples and course of UE during dehydration. Examples of transverse cuts, percentage distribution of 50-µm lumen area categories and ultrasonic emission energy in 5% steps of the cumulative number of UEs (relative UE) for Category I (a–c), Category II (d–f), Category III (g–i) and Category IV (j–l) specimens are given. Whiskers represent one standard error and reference bars 200 µm.

Europe PMC Funders Author Manuscripts

Europe PMC Funders Author Manuscripts

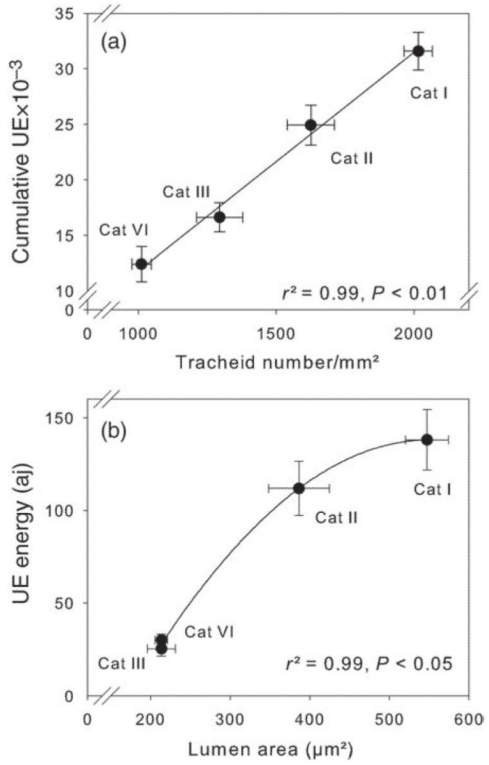

Figure 2.

Relationship of wood structure and UE parameters. Plots of tracheid number per square millimetre transverse surface versus cumulative number of UEs (a) and mean UE energy versus mean lumen area (b) of standard size wood splits are given. For description of categories (Categories I–IV), see Figure 1. Error bars represent one standard error. Significant relationships between traits are indicated by linear (a) and quadratic (b) regression lines.

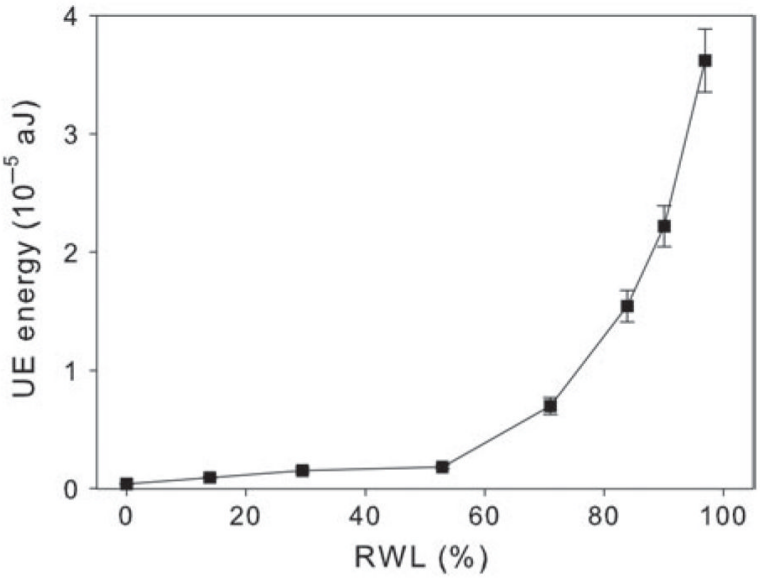

Figure 3.
Ultrasonic emission energy–moisture relationship. Ultrasonic emission energy was plotted against the relative water loss (RWL) of a mature Norway spruce wood beam (150 mm axial × 7 mm radial × 10 mm tangential). The variation in UE energy with increasing moisture loss was tested by the HSU-Nielsen lead break source (5 °mm, 2H) method. The distance between UE transducer and the acoustic source was 10 cm.

Europe PMC Funders Author Manuscripts

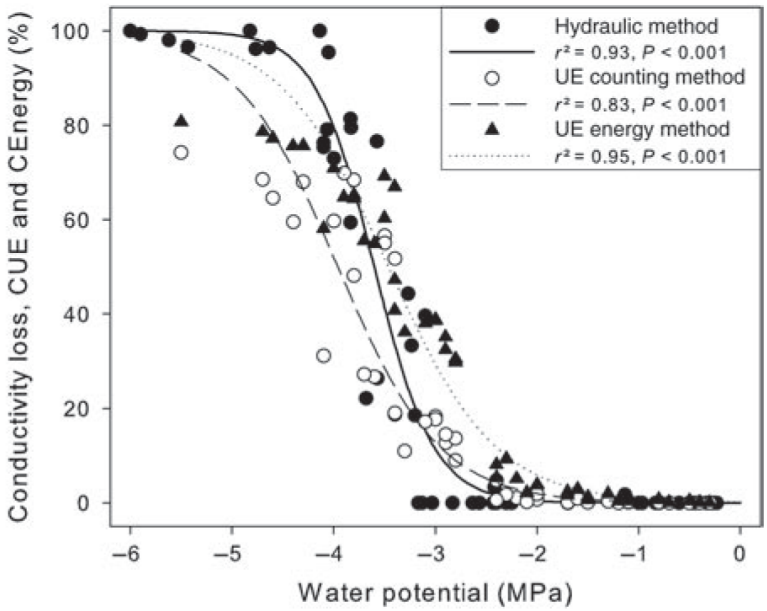

Figure 4.
Hydraulic and acoustic VCs. Percentage loss of conductivity (closed circles, solid line), percentage of cumulative number of UEs (CUE, open circles, dashed line) and percentage of cumulative ultrasonic emission energy (CEnergy, closed triangles, dotted line) plotted against water potential are shown. Curves were fitted with exponential sigmoidal equations.

Europe PMC Funders Author Manuscripts

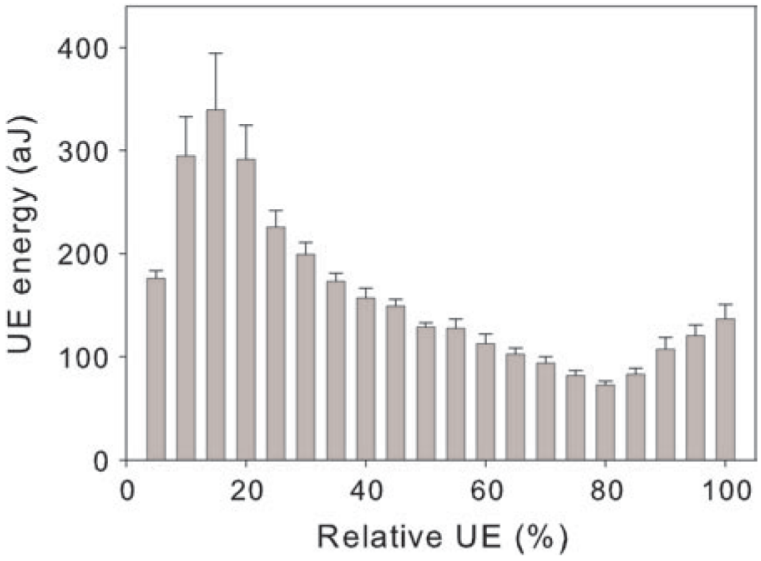

Figure 5.
Course of UE during dehydration of entire branches. Mean UE values in 5% steps of the cumulative number of UEs (relative UE) of two Norway spruce branches are given. Whiskers of the columns indicate one standard error.

Europe PMC Funders Author Manuscripts

Europe PMC Funders Author Manuscripts

Table 1

Anatomical and UE characteristics of wood splits.

	Category I	Category II	Category III	Category IV
Lumen area (μm^2)	547.2 ± 2 7 .0[c]	386.5 ± 38.3[b]	213.5 ± 1 7 .7[a]	213.4 ± 7. 9[a]
Lumen diameter radial (μm)	29.3 ± 0.7[c]	22.4 ± 1.8[b]	15.4 ± 0.5[a]	17.8 ± 0.4[a]
Lumen diameter tangential (μm)	23.6 ± 0.7[c]	20.5 ± 0.9[b]	15.7 ± 0.7[a]	15.3 ± 0.4[a]
Tracheids per cross-sectional area (number/mm^2)	1011.4 ± 35.2[a]	1295.1 ± 83.8[b]	1626.1 ± 85.8[c]	2016.0 ± 51.4[d]
Wood density (g/cm^3)	0.31 ± 0.01[a]	0.39 ± 0.03[a]	0.51 ± 0.03[b]	0.35 ± 0.01[a]
UE Energy (aJ)	138.0 ± 16.4[b]	111.8 ± 14.6[b]	25.4 ± 3.9[a]	30.0 ± 3.2[a]
Cumulative number of UE (10^{-3})	12.4 ± 1.6[a]	16.6 ± 1.3[a]	24.9 ± 1.7[b]	31.6 ± 1.7[b]
N	10	10	8	10

Split samples consisted of mature wood with quite uniform lumen diameters (Category I), of wood from the earlywood–latewood transition zone or of mature earlywood with 30–50% latewood from the previous annual ring (Category II), of mature wood with >50% latewood from the previous or the same annual ring (Category III) and of juvenile earlywood with quite uniform tracheid diameters (Category IV). Different letters indicate signifcant differences in the mean values.

Europe PMC Funders Author Manuscripts

Table 2

Pressure at 12 and 50% loss of conductivity and parameter *a* of vulnerability analysis on dehydrating twigs of *P. abies*.

	Hydraulic method	UE count	UE energy
P_{12} (MPa)	− 3.01 ± 0.11	− 2.88 ± 0.14[a]	− 2.24 ± 0.03[b]
P_{50} (MPa)	− 3.60 ± 0.04	− 3.87 ± 0.23[a]	− 3.46 ± 0.12[a]
Parameter *a*	3.4 ± 0.40	2.1 ± 0.1[a]	1.6 ± 0.1[a]
Branches (*n*)	52	3	3

VCs (Figure 4) were analysed from hydraulic measurements and from cumulative counts and cumulative energy of ultrasonic signals. Different letters indicate signifcant differences in the mean values of UE counts and energy. Statistical tests for the hydraulic method were not possible as statistical units differed from UE analysis (see text).